Acta of Bioengineering and Biomechanics
Vol. 15, No. 3, 2013

Original paper
DOI: 10.5277/abb130303

Modeling and stress analyses of a normal foot-ankle and a prosthetic foot-ankle complex

MUSTAFA OZEN[1]*, ONUR SAYMAN[1], HASAN HAVITCIOGLU[2]

[1] Faculty of Engineering, Dokuz Eylul University, Izmir, Turkey.
[2] Faculty of Medicine, Dokuz Eylul University, Izmir, Turkey.

Total ankle replacement (TAR) is a relatively new concept and is becoming more popular for treatment of ankle arthritis and fractures. Because of the high costs and difficulties of experimental studies, the developments of TAR prostheses are progressing very slowly. For this reason, the medical imaging techniques such as CT, and MR have become more and more useful. The finite element method (FEM) is a widely used technique to estimate the mechanical behaviors of materials and structures in engineering applications. FEM has also been increasingly applied to biomechanical analyses of human bones, tissues and organs, thanks to the development of both the computing capabilities and the medical imaging techniques. 3-D finite element models of the human foot and ankle from reconstruction of MR and CT images have been investigated by some authors. In this study, data of geometries (used in modeling) of a normal and a prosthetic foot and ankle were obtained from a 3D reconstruction of CT images. The segmentation software, MIMICS was used to generate the 3D images of the bony structures, soft tissues and components of prosthesis of normal and prosthetic ankle-foot complex. Except the spaces between the adjacent surface of the phalanges fused, metatarsals, cuneiforms, cuboid, navicular, talus and calcaneus bones, soft tissues and components of prosthesis were independently developed to form foot and ankle complex. SOLIDWORKS program was used to form the boundary surfaces of all model components and then the solid models were obtained from these boundary surfaces. Finite element analyses software, ABAQUS was used to perform the numerical stress analyses of these models for balanced standing position. Plantar pressure and von Mises stress distributions of the normal and prosthetic ankles were compared with each other. There was a peak pressure increase at the 4th metatarsal, first metatarsal and talus bones and a decrease at the intermediate cuneiform and calcaneus bones, in prosthetic ankle-foot complex compared to normal one. The predicted plantar pressures and von Misses stress distributions for a normal foot were consistent with other FE models given in the literature. The present study is aimed to open new approaches for the development of ankle prosthesis.

Key words: *3-D modeling, finite element analysis (FEA), prosthetic foot-ankle complex*

1. Introduction

Total ankle replacement is a relatively new concept and is becoming more popular for treatment of ankle arthritis and fractures. Literature about TAR describes generally good results [1]–[3]. Dyrby et al. [4] evaluated the function of the ankle joint during walking before and after Scandinavian Total Ankle Replacement (STAR). They investigated 2D net joint moments in nine patients. Houdijk et al. [5] determined the mechanical load and quasi-stiffness of the ankle joint during walking, after Total Ankle Replacement and compared the obtained results with the normal load and stiffness of a healthy ankle joint. Ten TAR patients and 10 healthy control subjects participated in this study. They reported that, despite small differences in internal work at the ankle, there was no significant difference in mechanical loading of the ankle after TAR. Almost all of the studies regarding the ankle prosthesis in the literature are in vivo studies. Because of the high costs and difficulties of experimental studies, the developments of prostheses are progressing very slowly. For this reason, imaging

* Corresponding author: Mustafa Ozen, Faculty of Engineering, Dokuz Eylul University, 35397 Buca, Izmir, Turkey. Tel: +90 232 3019256; fax: +90 232 3019204, e-mail: mustafa.ozen@deu.edu.tr

Received: July 23rd, 2012
Accepted for publication: March 7th, 2013

techniques have become more and more useful to characterize natural biomaterials. One of the most widely used techniques is the computed tomography (CT) that is preferred because of its high resolution. The finite element method (FEM) is a widely used technique to estimate the mechanical behaviors of materials and structures in engineering applications. FEM has also been increasingly applied to biomechanical analyses of human bones, tissues and organs, thanks to the development of both the computing capabilities and the medical imaging techniques such as CT and MRI [6]–[8]. Reggiani et al. [9] developed a finite element model of a 3 component TAR prosthesis. They analyzed the contact pressures and ligament forces during passive, i.e., virtually unloaded, and active, i.e., stance phase of gait conditions. They observed a peak contact pressure which is about 16.8 MPa. Viceconti et al. [10] used five mesh-generation methods to build a FEM model of a femur. They discussed the advantages and disadvantages of the method in terms of geometric adaptability, accuracy of the result and computational cost. Niebur et al [11] used voxel-based mesh generation to study the failure mechanism of trabecular bones. The method seems to be the easiest way of 3D element generation, highly automated and efficient. However, the obtained results are not satisfactory when the focus is on the stress/strain distributions near boundaries. Scifert et al. [12] used FEM to improve the design for resisting total hip dislocation. Tadepalli et al. [13] evaluated the performance of linear and quadratic tetrahedral and hexahedral elements under material incompressibility, frictional contact, and complex loading conditions. They demonstrated that for a range of simulation conditions, hybrid hexahedral elements consistently performed well while hybrid linear tetrahedral elements performed poorly. Tadepalli et al. [14] presented a general framework for computer-aided planning of orthopedic interventions based on finite element modeling via the reconstruction of the patient's anatomy from 3D image datasets. They developed a prototype program. They also demonstrated a simulation and meshing of a cervical laminoplasty procedure. A meshing technique for generating hexahedral FE models was developed by Devries et al. [15]. They compared their technique to widely accepted meshing methods. They used experimental studies to validate their mesh definitions. Even more relevant reports [16]–[18] can be found in literature. 3-D finite element models of the human foot and ankle from reconstruction of MR and CT images have been developed by some authors. Gefen et al. [19] developed a complex three-dimensional FE model of a normal foot structure, including cartilage and ligaments. They modeled each of the discrete events during the stance phase of gait, individually for analyses. In order to obtain information of the relationship between the foot skeleton motion during stance and the resultant foot–ground pressure pattern, a novel experimental gait analysis technique was developed and used in their study. Chen et al. [20] presented a 3-D finite element model of a normal foot, to examine the stress distribution during mid-stance to push-off phase during barefoot gait. They used computed tomography (CT) sectional images to identify the major bones and soft tissues of the foot for construction of the finite element foot model. Chen et al. [21] established a 3-D nonlinear finite element model of a human foot complex together with comprehensive skeletal and soft-tissue components. The model was validated by experimental data of subject-specific barefoot plantar pressure measurements. By the model, 3-D, internal, plantar soft-tissue deformations and stresses were investigated. Cheung et al. [22] developed a comprehensive FE model of the foot and ankle, using 3D actual geometry of both skeletal and soft tissues components. They have investigated the effect of soft tissue stiffness on the plantar pressure distributions and the internal load transfer among bony structures. Even more relevant reports [23]–[30] can be found in literature. Jacob and Patil developed a 3-D, two-arch model of the foot from the X-rays. They took foot geometry from a normal and a Hansen's disease subject [31], and normal and diabetic subjects [32], including bones, cartilages, ligaments, important muscle forces, and foot-sole soft-tissue. They carried out stress analysis by finite element technique for quasi-static walking phases of heel-strike, mid-stance, and push-off. They reported that the highest stress occur during push-off phase in the dorsal central part of the lateral and medial metatarsals, the dorsal junction of the calcaneus, and the cuboid and plantar central part of the lateral metatarsals in the foot. The first objective of this study was to generate models of normal and prosthetic ankle-foot complex bones, soft tissues and components of prosthesis, by using CT images and MIMICS (Materialise) software and SOLIDWORKS software. The second purpose was to export this model into ABAQUS codes, a finite element software, and hence to analyze the stress and contact pressure distribution of the models. In the FEM models for normal ankle, interactions between bones to cartilages, and soft tissues to ground supports were considered as sliding contact parts while interactions between the soft tissues and bone surfaces were defined as tied contacting parts. In addition, for prosthetic ankle sliding contacts were

defined between the components of prosthesis and tibia and talus. For balanced standing position stress and plantar pressure distribution of the normal and prosthetic ankles were compared in the light of numerical analysis results.

The CT machine, SOLIDWORKS software and ABAQUS software used in this study were provided by Dokuz Eylul University (Izmir, Turkey) and MIMICS software used in this study was provided by 4C Medical (Istanbul, Turkey).

2. Materials and methods

The first objective of this study was to obtain 3D CT images of the ankle-foot complex in order to construct the 3-D finite element models. In CT, the data is encoded in the Digital Imagining and Communications in Medicine (DICOM) format. The 3-D bone models were then generated by using MIMICS and SOLIDWORKS software from the data mentioned. The solid model was then imported and assembled in the FE package ABAQUS. To show the difference between normal and prosthetic foot-ankle complex, CT images of a patient with a prosthetic foot was used. Therefore, the geometry of the FE model was obtained from 3-D reconstruction of CT images from the right foot (normal) and left foot (prosthetic) of a male patient of age 40, height 170 mm and mass 80 kg. CT images were taken with intervals of 0.9 mm in the neutral unloaded position.

2.1. Modeling of the ankle-foot complex

Firstly, the DICOM images were exported to MIMICS program. The bony structures, soft tissues and components of prosthesis were separated by defining different threshold values in the program. Thus 3D images of bony structures, soft tissues and prosthesis components were independently developed. At the segmentation process, the spaces between the phalanges were fused due to failure of interphalangeal joints. The 3D images of the right (normal) foot consisted of 5 fused phalanges, 5 metatarsals, 3 cuneiform, cuboid, navicular, talus, fibula, tibia and calcaneus bones and soft tissue. Thus, 3D images of normal foot-ankle complex consisted of these 20 components. However, for prosthetic foot-ankle complex, 3D images of three components of prosthesis were also independently developed. Thus, prosthetic foot-ankle complex consisted of 23 components. Point clouds of all of the segmented 3D images were exported to the SOLIDWORKS program. The boundary surfaces of the bones, soft tissues and prosthesis components were processed by using the Mesh Prep Wizard tool of the program. For simplification of complex surfaces, global smoothness was applied to all components, and then the surfaces were created. To construct the cartilages, solid parts were generated between the adjacent surfaces of all joint bones. Bones, cartilages and components of prosthesis were subtracted from the defined full soft tissue to form the encapsulated soft tissue. After having adequate surfaces, solid models were obtained. A horizontal plate tangent to planar surface of the soft tissue was also generated to simulate the ground support. All of the solid parts were saved in Para Solid format and imported to ABAQUS program. A flow chart of the modeling and analysis methodology of 3D models is given in Fig. 1.

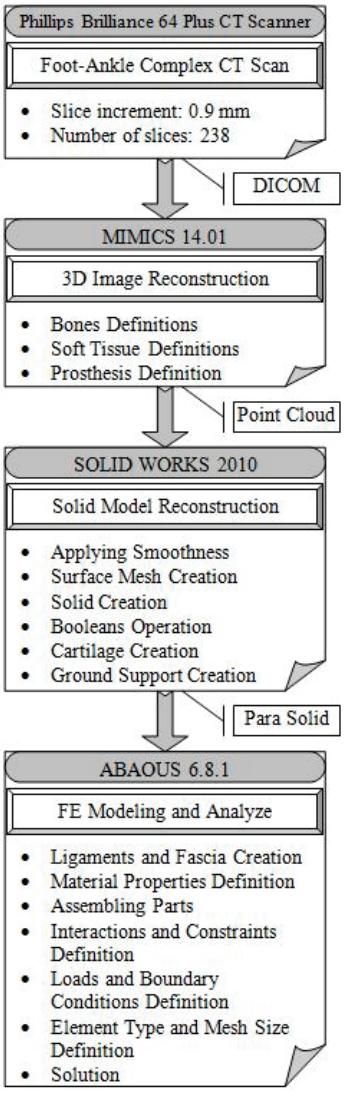

Fig. 1 Methodology of modeling and analysis

2.2. FEA of the ankle-foot complex

A finite element analysis package ABAQUS was used to perform the finite element analysis. Firstly, the imported parts were assembled by the program to obtain the model. A total number of 76 ligaments and plantar fascia were defined for normal foot by connecting points on the bones. However, for prosthetic foot except the anterior tibiofibular, interroseous tibiofibular, anterior talofibular, posterior tibiofibular and transverse tibiofibular ligaments (cut at the implantation of prosthesis) a total number of 71 ligaments and plantar fascia were defined. All of the ligaments and plantar fascia were defined by connecting the corresponding attachment points on the bones obtained from the Interactive Foot and Ankle [Primal Picture Ltd., London U.K., 2009]. The plantar fascias were divided into 5 rays of separate sections, between the calcaneus and the metatarsophalangeal joints. 3D models of normal and prosthetic foots are shown in Fig. 2.

Except the soft tissue, all other components of models were assumed as homogeneous, isotropic and linearly elastic materials. Young's modulus and Poisson's ratio for the bony structures were selected as 7300 MPa and 0.3, respectively, by weighting the cortical and trabecular properties of bones based on the model developed by Gefen et al. [19]. Young's modulus and Poisson's ratio of the cartilage [33], ligaments [34] and the plantar fascia [35] were selected from the literature, Table 1. The ligaments and fascia were assumed to be incompressible. The soft tissues were described by hyper elastic behavior with material properties adopted from previous literature [22], Table 2. Material properties of concrete were assumed for ground support.

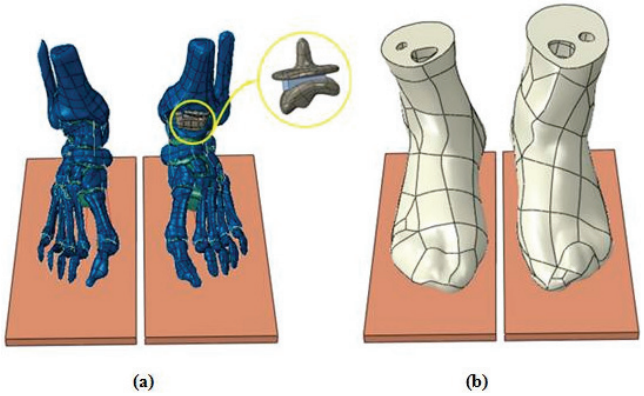

Fig. 2. 3D model of ground support:
(a) bone structure, cartilage, ligaments, fascia,
and components of prosthesis, (b) soft tissue

The Bueshel Pappas Total Ankle Replacement system was used in this study, which consisted of

Table 1. Material properties and element types of the anatomical parts of the finite element model

Component	Young's modulus (MPa)	Poisson's ratio	Element type	Cross sectional area (mm^2)
Bones	7300	0.3	3D-tetrahedral	
Soft tissue	Hyper elastic		3D-tetrahedral	
Cartilage	10	0.4	3D-tetrahedral	
Ligaments	260	0.4	Tension-only truss	18.4
Plantar fascia	350	0.4	Tension-only truss	58.6

Table 2. The coefficients of the hyperelastic material used for the soft tissue

C_{10}	C_{01}	C_{20}	C_{11}	C_{02}	D_1	D_2
0.08556	–0.05841	0.039	–0.02319	0.00851	3.65273	0

Table 3. Material properties and element types of the prosthesis components and ground support

Component	Material	Young's modulus (MPa)	Poisson's ratio	Element type
Talar and tibial	Cobalt-chromium-molybdenum (Co-Cr-Mo)	220000	0.3	3D-tetrahedral
Mobile bearing	Ultra-high molecular weight polyethylene (UHMWPE)	600	0.46	3D-tetrahedral
Ground support	Concrete	17000	0.1	3D-brick

three components: tibial component, talar component and an interlaying mobile bearing. Tibial and talar components of prosthesis were made of cobalt chromium molybdenum (Co-Cr-Mo). Therefore, Young's modulus and Poisson's ratio for this material were chosen as 220 GPa and 0.3, respectively. Bearing component was made of ultra high molecular weight polyethylene (UHMWPE). Young's modulus and Poisson's ratio for this material were chosen as 600 MPa and 0.46, respectively, Table 3.

In order to simulate the interactions between the bone-to-cartilage, bone-to-soft tissue, soft tissue-to-plate, prosthesis component-to-component, and prosthesis component-to-bone (tibia and talus) the surface to surface contact algorithm of ABAQUS is utilized. The contact between the bone and cartilages is assumed to be frictionless due to lubricating nature of the articulating surfaces. The soft contact behavior of the articular cartilages was simulated by a contact stiffness defined by Athanasiou et al. [33]. A frictional contact between the planar surface of foot and ground support was defined with a coefficient of friction 0.6 [36]. Usually, the soft tissue is adherent to the underlying bone so that a tied contact was defined between the surface of the bones and inner surface of the soft tissue. The contact between the talar and tibial components of prosthesis and talus and tibia was defined as frictionless one. The contact between the polyethylene and metal components was also assumed to be frictionless [9]. The bony, soft tissues and components of prosthesis were meshed with tetrahedral elements, while the ground support was meshed with 3D brick elements and ligaments and plantar fascia were defined by tension only truss elements. For a subject with body mass of 80 kg, a vertical force of approximately 400 N is applied on each foot during balanced standing. The body weight was applied as concentrated forces at the underneath surface of the plate. The Achilles tendon force was set as 75% of the total plantar force on the foot, based on the studies showing that this setting provided the closest result between measured and predicted centre of pressure during balanced standing [25]. The Achilles tendon forces were represented by five equivalent force vectors at the posterior extreme of the calcaneus. The proximal ends of the tibia and fibula and superior surface of the soft tissue were fixed throughout the analysis. The same loading and boundary conditions were considered for normal foot-ankle and prosthetic foot-ankle models in the finite element analysis. Boundary and loading conditions of FE model is shown in Fig. 3.

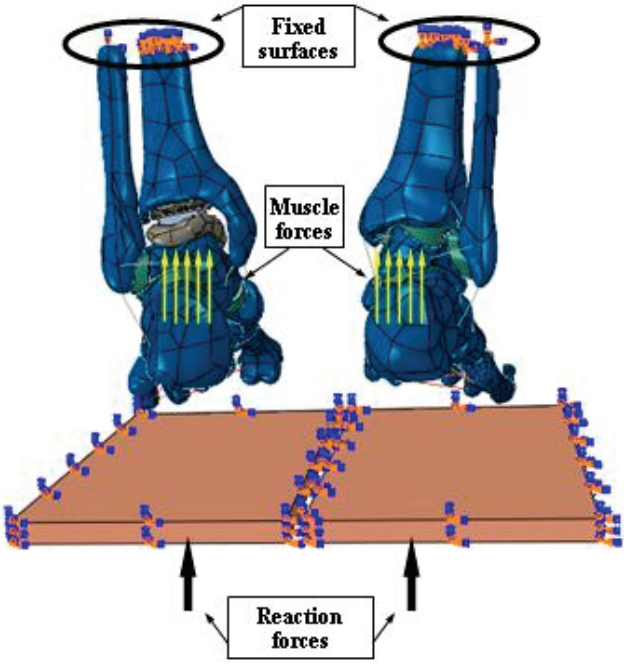

Fig. 3. Boundary and loading conditions of FE model

3. Results

A geometrically accurate 3D finite element model of a normal foot-ankle and a prosthetic foot-ankle complex of a patient was developed. The FEM model created enables the stress/strain distribution to be predicted under balanced standing position. In the analysis, the von Mises equivalent stress distributions and planar pressures were examined. From the analysis, equivalent stress distribution in each of the foot bones and planar pressure in the plantar surface of the soft tissue were obtained for both normal foot-ankle and prosthetic foot-ankle models considering balanced standing. For the validation of the model, the predicted plantar pressure of the current FE model is compared with those of experimental data and other FE results given in literature, Fig. 4. As seen in the figure, the position and peak value of stress concentration are comparable and are in good agreement. The FE predicted plantar pressure distribution of normal and prosthetic models are also given in the figure. The difference in pressure distribution is significant between normal and prosthetic foot. It is seen that for the normal foot model, the peak plantar pressure, about 0.159 MPa, occurs at the rear foot (heel) and forefoot (the first, third and fifth metatarsals head regions), while the corresponding predicted peak pressure for prosthetic foot is about 0.192 MPa locating at the forefoot (the first and fifth metatarsal head re-

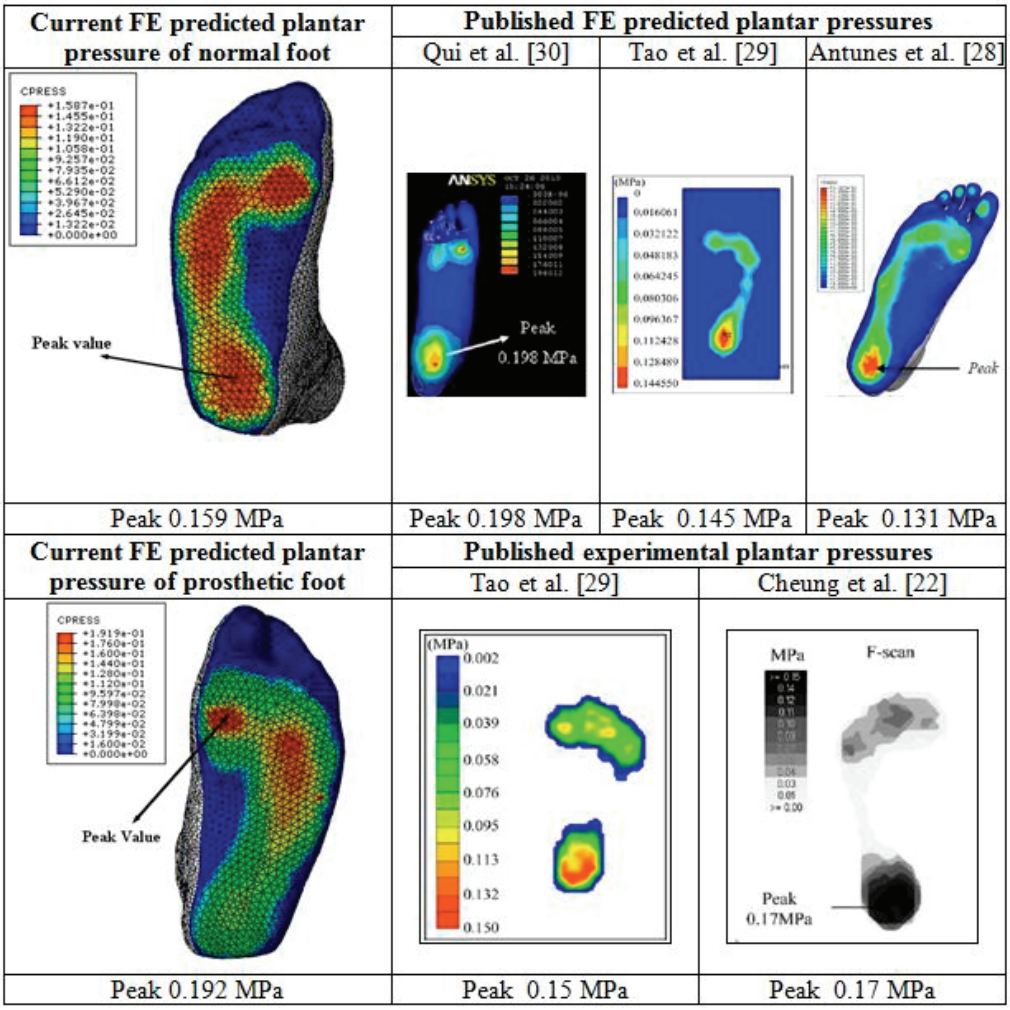

Fig. 4. Comparison of predicted plantar pressures with published FE predicted and experimental data

gions). The von Mises stress of dorsal soft tissue around ankle joints increased from 0.01 MPa to 0.03 MPa on average.

The predicted von Mises stress distributions of bony structures for both models are given in Fig. 5. As seen in the figure, the dorsal surface at the midshafts of the third to fifth metatarsals and the dorsal surface of the talus and tibia exposed higher stress concentration for prosthetic foot, while the midshaft of the second to fourth metatarsals sustained high stress for normal foot during balanced standing. Regarding joint stress distributions, for normal foot, a peak von Mises stress of about 6.766 MPa is found to be at the 3rd metatarsal, followed by 5.50 MPa at the tibia, 3.464 MPa at the calcaneus, and 3.371 MPa at the 2nd metatarsal. For prosthetic foot-ankle complex, the peak values are respectively, 7.560 MPa at tibia, 5.58 MPa at the 4th metatarsal and 4.794 MPa at the 5th metatarsal. Analysis results showed that an increase in equivalent stresses of the 4th metatarsal, 1st metatarsal and talus for prosthetic foot-ankle occurs, compared to a normal foot-ankle. On the contrary, a decrease in those stresses of intermediate cuneiform, calcaneus and the 3rd metatarsal is observed. The peak von Mises stress values are depicted in Table 4, for comparison.

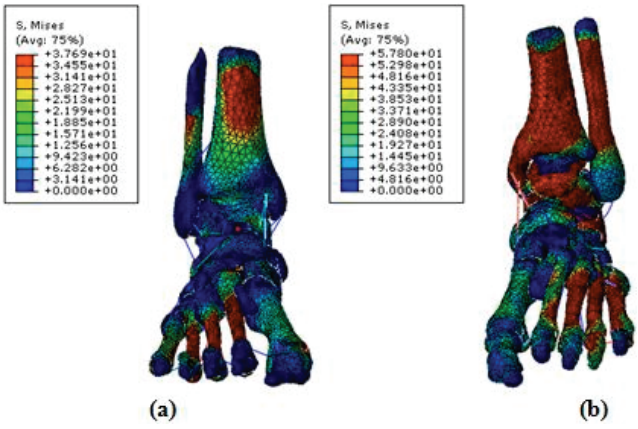

Fig. 5. Von Mises stress distribution of (a) normal foot, (b) prosthetic foot

Table 4. The FE predicted peak von Mises stress in the normal and prosthetic foot bones during balanced standing

Bone	Peak von Mises stresses (MPa)	
	normal	prosthetic
Tibia	5.550	7.560
Fibula	1.267	2.684
Talus	2.068	4.730
Calcaneus	3.464	2.302
Navicular	1.697	2.080
Cuboid	1.134	1.621
Medial cuneiform	0.914	1.050
Intermediate cuneiform	1.205	0.118
Lateral cuneiform	2.352	2.947
1st metatarsal	1.300	3.196
2nd metatarsal	3.371	4.639
3rd metatarsal	6.766	4.536
4th metatarsal	2.000	5.580
5th metatarsal	2.240	4.794
1st toe	0.584	0.567
2nd toe	0.496	0.551
3rd toe	0.552	0.916
4th toe	0.307	0.451
5th toe	0.131	0.190

4. Discussion

Total ankle replacement is one of the most common treatment methods of ankle arthritis and fractures. Knowledge about the stress distribution of the foot-ankle complex is a very important point for development of the prosthesis. Because of the high costs and difficulties of direct measurement of stress distribution of foot-ankle complex, the uses of a FE model have become more useful. In this study, the CT images of a patient normal (left) and prosthetic (right) foot were used to obtain a 3D finite element model of the ankle-foot complex. Then, for normal foot-ankle and prosthetic foot-ankle models, a numerical stress analysis was carried out. The main objective of this work was to compare the von Mises stress and planar pressure distributions of ankle-foot complex in a normal foot-ankle and prosthetic foot-ankle of a patient during balanced standing. In the current study, cortical and cancellous bones were modeled as single homogeneous components with linear elastic properties. The material properties of the bone, prosthesis components, ligaments, and fascia were assumed to be linear and are of elastic behavior. For the validation of the FE model, all current material properties were selected according to literature. Static loading conditions were considered in the analysis. Some simplifications on the geometry and material properties in modeling of both a normal foot-ankle and a prosthetic foot-ankle were done in order to reduce the complexity of the model. And also only the Achilles tendon force was considered while other intrinsic and extrinsic muscle forces were not simulated. The current model may assist pre-treatment planning and design of ankle prosthesis. The predicted equivalent stress and planar pressure distributions for a normal foot are in good agreement with the other FE models and experimental results of normal foot for balanced standing position given in the literature. For instance, Cheung et al. [22] have predicted relatively higher equivalent stresses at the mid-shaft of metatarsals, as 7.94 and 4.47 MPa in the third and second metatarsals, respectively. The values seem to be higher than the values obtained in the present study. In spite of the differences in stress intensities, however, the stress distributions obtained are in good agreement with those of literature. Plantar pressure distribution measurement has been widely used for validation of FE models, [21]–[23], [27]–[30]. In this study, plantar contact pressure under balanced standing loading condition was recorded with the FE prediction. There is good agreement between the overall shapes of contact patterns of predicted and measured plantar pressure distribution.

The analysis results showed that the stresses in rear foot of the prosthetic foot-ankle increase to a normal foot-ankle. Whereas, the equivalent stresses of fore foot are decreased. Analysis results and patient complaints are found to be consistent with each other. For instance, the higher stress variations in the prosthetic foot-ankle model compared to a normal foot-ankle were in third to fifth metatarsals, talus and tibia, where the patient complaints focused on. Based on the current study, more advanced finite element models can be created. Therefore, geometry of the prosthesis may be modified efficiently by using the analysis results.

The current method is cheaper and easier than the direct measurement techniques for analyzing the stress and pressure distributions of both normal and prosthetic foot-ankle complex. The method may assist pretreatment planning and design of the total ankle replacement. Also geometry and material properties of the prosthesis components can be changed and the effects of these changes can be investigated easily. The biomechanical effects of the other factors on the stress distribution of both normal and prosthetic foots can be investigated.

Some simplifications on the geometry, material properties and loadings of the bones, soft tissues, ligaments and muscles were made to reduce the complexity of the model. These simplifications may affect

the estimated stress results, however, the stress distribution and values showed good agreement with previous measurement results from literature.

References

[1] ANDERSON T., MONTGOMERY F., CARLSSON A., *Uncemented STAR total ankle prostheses. Three to eight-year follow-up of fifty-one consecutive ankles*, The Journal of Bone and Joint Surgery AM, 2003, Vol. 85, 1321–1329.

[2] WOOD P.L., DEAKIN S., *Total ankle replacement. The result in 200 ankles*, The Journal of Bone and Joint Surgery BR, 2003, Vol. 85, 334–341.

[3] AJAI S., *A review of the STAR prosthetic system and the biomechanical considerations in total ankle replacements*, Foot and Ankle Surgery, 2011, Vol. 17, 64–67.

[4] DYRBY C., CHOU L.B., ANDRIACCHI T.P., MANN R.A., *Functional evaluation of the Scandinavian Total Ankle Replacement*, Foot & Ankle International, 2004, Vol. 25, 377–381.

[5] HOUDIJK H., DOETS H.C., van MIDDELKOOP M., VEEGER H.E.J., *Joint stiffness of the ankle during walking after successful mobile-bearing total ankle replacement*, Gait & Posture, 2008, Vol. 27, 115–119.

[6] PRENDERGAST P.J., *Finite element models in tissue mechanics and orthopaedic implant design*, Clinical Biomechanics, 1997, Vol. 12, 343–366.

[7] ZHNAG M., MAK A., ROBERTS V.C., *Finite element modeling of a residual lower-limb in a prosthetic socket: a survey of the development in the first decade*, Medical Engineering & Physics, 1998, Vol. 20, 360–373.

[8] SCHULLER-GÖTZBURG P., KRENKEL C., *2D-finite element analyses and histomorphology of lag screws with and without a biconcave washer*, Journal of Biomechanics, 1999, Vol. 32, 511–520.

[9] REGGIANI B., LEARDINI A., CORAZZA F., TAYLOR M., *Finite element analysis of a total ankle replacement during the stance phase of gait*, Journal of Biomechanics, 2006, Vol. 39, 1435–1443.

[10] VICECONTI M., BELLINGERI L., CRISTOFOLINI L., TONI A., *A comparative study on different methods of automatic mesh generation of human femurs*, Medical Engineering & Physics, 1998, Vol. 20, 1–10.

[11] NIEBUR G.L., FELDSTEIN M.J., YUEN J.C., CHEN T.J., KEAVENY T.M., *High-resolution finite element models with tissue strength asymmetry accurately predict failure of trabecular bone*, Journal of Biomechanics, 2000, Vol. 33, 1575–1583.

[12] SCIFERT C.F., BROWN T.D., LIPMAN J.D., *Finite element analysis of a novel design approach to resisting total hip dislocation*, Clinical Biomechanics, 1999, Vol. 14, 697–703.

[13] TADEPALLI S.C., ERDEMIR A., CAVANGH P.R., *Comparison of hexahedral and tetrahedral elements in finite element analysis of the foot and footwear*, Journal of Biomechanics, 2011, Vol. 44, 2337–2343.

[14] TADEPALLI S.C., SHIVANNA K.H., MAGNOTTA V.A., KALLEMEYN N.A., GROSLAND N.M., *Toward the development of virtual surgical tools to aid orthopaedic FE analyses*, Journal on Advances in Signal Processing, 2010, 1902931–1902937.

[15] DEVRIES N.A., SHIVANNA K.H., TADEPALLI S.C., MAGNOTTA V.A., GROSLAND N.M., *Ia-FEMesh: anatomic FE models – a check of mesh accuracy and validity*, The Iowa Orthopaedic Journal, 2009, Vol. 29, 48–54.

[16] CHENG C.K., CHEN H.H., KUO H.H., LEE C.L., CHEN W.J., LIU C.L., *A three-dimensional mathematical model for predicting spinal joint force distribution during manual liftings*, Clinical Biomechanics, 1998, Vol. 13, 59–64.

[17] BANDAK F.A., TANNOUS R.E., TORIDIS T., *On the development of an osseo-ligamentous finite element model of human ankle joint*, International Journal of Solids and Structures, 2001, Vol. 38, 1681–1697.

[18] BARTOS M., KESTRANEK Z., NEDOMA J., STEHLIK J., *On the 2D and 3D finite element simulation in orthopaedy using MRI*, Mathematics and Computers in Simulation, 1999, Vol. 50, 115–121.

[19] GEFEN A., MEGIDO-RAVID M., ITZCHAK Y., ARCAN M., *Biomechanical Analysis of the Three-Dimensional Foot Structure during Gait: A Basic Tool for Clinical Applications*, Journal of Biomechanical Engineering, 2000, Vol. 12, 631–639.

[20] CHEN W.M., LEE T., LEE P.V.S., LEE J.W., LEE S.J., *Effects of internal stress concentrations in plantar soft-tissue – A preliminary three-dimensional finite element analysis*, Medical Engineering & Physics, 2010, Vol. 32, 324–331.

[21] CHEN W.P., TANG F.T., JU C.W., *Stress Distribution of the Foot During Mid-stance to Push-off in Barefoot Gait: a 3-D Finite Element Analysis*, Clinical Biomechanics, 2001, Vol. 16, 614–620.

[22] CHEUNG J.T.M., ZHANG M., LEUNG A.K.L., FAN Y.B., *Three-dimensional finite element analysis of the foot during standing – a material sensitivity study*, Journal of Biomechanics, 2005, Vol. 38, 1045–1054.

[23] CHEUNG J.T.M., ZHANG M., AN K.N., *Effects of plantar fascia stiffness on the biomechanical responses of the ankle-foot complex*, Clinical Biomechanics, 2004, Vol. 19, 839–846.

[24] CHEUNG J.T.M., ZHANG M., *Finite element modeling of the human foot and footwear*, ABAQUS Users Conference, May 23, 2006, Cambridge, MA USA.

[25] CHEUNG J.T.M., ZHANG M., AN K.N., *Effect of Achilles tendon loading on plantar fascia tension in the standing foot*, Clinical Biomechanics, 2006, Vol. 21, 194–203.

[26] CHEUNG J.T.M., ZHANG M., *Parametric design of pressure-relieving foot orthosis using statistical-based finite element method*, Medical Engineering & Physics, 2008, Vol. 30, 269–277.

[27] YU J., CHEUNG J.T.M., FAN Y., ZHANG Y., LEUNG A.K.L., ZHANG M., *Development of a finite element model of female foot for high-heeled shoe design*, Clinical Biomechanics, 2008, Vol. 23, 31–38.

[28] ANTUNES P.J., DIAS G.R., COELHO A.T., REBELO F., PEREIRA T., *Non-linear finite element modeling of anatomically detailed 3D foot model*, Materialise, http://materialise.com/materialise/view/ en/394365-Non-Linear + Finite + Element + Modeling + of + Anatomically + Detailed + 3D + Foot + Model.html, Retrieved 2012.

[29] TAO K., WANG D., WANG C., WANG X., LIU A., NESTER C.J., HOWARD D., *An in vivo experimental validation of a computational model of human foot*, Journal of Bionic Engineering, 2009, Vol. 6, 387–397.

[30] QIU T.X., TEO E.C., YAN Y.B., LEI W., *Finite element modeling of a 3D coupled foot–boot model*, Medical Engineering & Physics, 2011, Vol. 33, 1228–1233.

[31] JACOB S., PATIL M.K., *Three-dimensional foot modeling and analysis of stress in normal and early stage Hansen's disease with muscle paralysis*, Journal of Rehabilitation Research & Development, 1999, Vol. 36, 252–263.

[32] JACOB S., PATIL M.K., *Stress analysis in three-dimensional foot of normal and diabetic neuropathy*, Frontiers of Medical and Biological Engineering, 1999, Vol. 9, 211–227.

[33] ATHANASIOU K.A., LIU G.T., LAVERY L.A., LANCTOT D.R., SCHENCK R.C., *Biomechanical topography of human articular cartilage in the first metatarsophalangeal joint*, Clinical Orthopaedics and Related Research, 1998, Vol. 348, 269–381.

[34] SIEGLER S., BLOCK J., SCHNECK C.D., *The mechanical characteristics of the collateral ligaments of the human ankle joint*, Foot & Ankle, 1988, Vol. 8, 234–242.

[35] WRIGHT D., RENNELS D., *A study of the elastic properties of plantar fascia*, The Journal of Bone and Joint Surgery AM, 1964, Vol. 46, 482–492.

[36] ZHANG M., MAK A.F.T., *In vivo skin frictional properties*, Prosthetics and Orthotics International, 1999, Vol. 23, 135–141.